PCP
PLANT & CELL PHYSIOLOGY

Special Focus Issue – Regular Paper

VAN4 Encodes a Putative TRS120 That is Required for Normal Cell Growth and Vein Development in *Arabidopsis*

Satoshi Naramoto[1,2,*], Tomasz Nodzyński[3], Tomoko Dainobu[1], Hirotomo Takatsuka[4], Teruyo Okada[1], Jiří Friml[3,5] and Hiroo Fukuda[1]

[1]Department of Biological Sciences, Graduate School of Science, University of Tokyo, 7-3-1 Hongo, Bunkyo-ku, Tokyo, 113-0033 Japan
[2]Department of Life Science, International Christian University, Mitaka-shi, Tokyo, 181-8585 Japan
[3]Mendel Centre for Plant Genomics and Proteomics, Central European Institute of Technology (CEITEC), Masaryk University (MU), CZ-625 00, Brno, Czech Republic
[4]Graduate School of Biological Sciences, Nara Institute of Science and Technology, Nara, 630-0192 Japan
[5]Institute of Science and Technology Austria (IST), 3400 Klosterneuburg, Austria
*Corresponding author: E-mail, naramoto@biol.s.u-tokyo.ac.jp; Fax, 81-3-5841-4462.
(Received August 30, 2013; Accepted January 8, 2014)

Leaf venation develops complex patterns in angiosperms, but the mechanism underlying this process is largely unknown. To elucidate the molecular mechanisms governing vein pattern formation, we previously isolated *vascular network defective* (*van*) mutants that displayed venation discontinuities. Here, we report the phenotypic analysis of *van4* mutants, and we identify and characterize the *VAN4* gene. Detailed phenotypic analysis shows that *van4* mutants are defective in procambium cell differentiation and subsequent vascular cell differentiation. Reduced shoot and root cell growth is observed in *van4* mutants, suggesting that *VAN4* function is important for cell growth and the establishment of venation continuity. Consistent with these phenotypes, the *VAN4* gene is strongly expressed in vascular and meristematic cells. *VAN4* encodes a putative TRS120, which is a known guanine nucleotide exchange factor (GEF) for Rab GTPase involved in regulating vesicle transport, and a known tethering factor that determines the specificity of membrane fusion. VAN4 protein localizes at the *trans*-Golgi network/early endosome (TGN/EE). Aberrant recycling of the auxin efflux carrier PIN proteins is observed in *van4* mutants. These results suggest that VAN4-mediated exocytosis at the TGN plays important roles in plant vascular development and cell growth in shoot and root. Our identification of VAN4 as a putative TRS120 shows that Rab GTPases are crucial (in addition to ARF GTPases) for continuous vascular development, and provides further evidence for the importance of vesicle transport in leaf vascular formation.

Keywords: *Arabidopsis* • Cell growth • Guanine nucleotide exchange factor (GEF) • Leaf venation pattern • Vascular cell differentiation • Vesicle trafficking.

Abbreviations: ARF, ADP-ribosylation factor; BAC, bacterial artificial chromosome; BFA, brefeldin A; DAG, days after germination; EE, early endosome; GAP, GTPase-activating protein; GEF, guanine nucleotide exchange factor; GFP, green fluorescent protein; GUS, β-glucuronidase; mRFP, monomeric red fluorescent protein; NPA, 1-*N*-naphthylphthalamic acid; PED, PIN1–GFP expression domain; PIN, PIN-FORMED; PM, plasma membrane; PVC/MVB, pre-vacuolar compartment/multivesicular body; RACE, rapid amplification of cDNA ends; TGN, *trans*-Golgi network; VAN4, Vascular Network Defective 4; VHA1, Vacuolar H^+-ATPase subunit 1.

Introduction

Vascular plants have a complex vascular structure composed of xylem and phloem. The vascular structure provides physical strength that enables plants to grow against gravity, and provides a network for the transport of water, minerals, photosynthate and signal molecules that enables plants to conquer non-aquatic environments. The vasculature network has a very complex structure, and a variety of leaf vascular network patterns are recognized among different species and organs. Despite this diversity, the successful use of leaf vein patterns as a species-specific diagnostic feature indicates that the patterning processes must be genetically regulated, and suggests that a common basic mechanism underlies the spatial arrangement of vascular cells.

Vascular cells originate from procambium cells; thus, the vein pattern is determined by the spatially regulated differentiation of procambium cells. The auxin canalization model has been proposed as a developmental mechanism that specifies procambium patterning (Sachs 1981, Sachs 1989, Sachs 1991). The auxin canalization model assumes that an initially homogeneous field emanates from an auxin source. Random fluctuation in auxin concentration in this field exposes some cells to

Plant Cell Physiol. 55(4): 750–763 (2014) doi:10.1093/pcp/pcu012, available online at www.pcp.oxfordjournals.org

higher auxin concentrations, leading to increased efficiency of auxin transport. These cells transport auxin to neighboring cells. This system reiteratively promotes auxin transport, which leads to canalization of auxin flow along a narrow file. The cells of the narrow file differentiate into procambium cells.

A number of studies indicate that auxin signaling and transport play important roles in vascular pattern formation (Nelson and Dengler 1997, Sieburth 1999, Berleth et al. 2000, Sachs 2000, Aloni 2001). These studies support the auxin canalization model. PIN-FORMED (PIN) proteins are identified as auxin efflux carriers that localize in a polar manner at plasma membranes (PMs); this polar localization determines the direction of auxin flow within the tissues (Petrášek et al. 2006, Wiśniewska et al. 2006). Mutation of *PIN1* causes a reduction in polar auxin transport and results in aberrant venation patterns (Mattsson et al. 1999, Koizumi et al. 2005). Detailed observations of PIN1–green fluorescent protein (GFP) localization during venation development clearly demonstrates the formation of procambium along routes of sustained polar auxin transport (Scarpella et al. 2006). Defective vein formation is also observed in auxin signaling mutants, such as *monopteros* (*mp*), and in seedlings treated with auxin transport inhibitors (Hardtke and Berleth 1998, Mattsson et al. 1999). The frequent association of defective auxin signaling or transport with aberrant vascular patterns strongly suggests a primary role for auxin in establishing shoot vascular patterns.

The subcellular localization of PIN proteins is determined by vesicle trafficking. Treatment with brefeldin A (BFA), an inhibitor of ADP ribosylation factor-guanine nucleotide exchange factor (ARF-GEF), causes the depletion of PIN proteins from the PM and their accumulation in endosomes called BFA bodies (Geldner et al. 2001). This effect is completely reversible, which indicates a continual transport of PIN proteins between endosomes and the PM (Geldner et al. 2001, Dhonukshe et al. 2007). Molecular processes mediating membrane transport systems, including vesicle formation, movement, tethering and fusion, are regulated by the large protein family of small GTPases that includes ARF and Rab (Zerial and McBride 2001, D'Souza-Schorey and Chavrier 2006). These small GTPases function through a cycle of GTP binding and GTP hydrolysis, which generates the GTP-bound active form and the GDP-bound inactive form. This cycle is spatio-temporally controlled by GEFs and GTPase-activating proteins (GAPs). GEFs promote the exchange of bound GDP for GTP, whereas GAPs stimulate GTP hydrolysis and counteract GEF activity. Consistent with this system, GNOM ARF-GEF is the target of BFA and functions in the translocation of proteins from endosomes to the PM (Geldner et al. 2003), and assists endocytic processes at the PM (Naramoto et al. 2010). Genetic screening of mutants that show defects in the BFA-induced intracellular accumulation of PIN1–GFP identified BEN1 (an ARF-GEF) and BEX5/RabA1b (a small GTPase) as regulators of endocytic recycling of PIN proteins (Tanaka et al. 2009, Asaoka et al. 2012, Feraru et al. 2012). These results clearly show that membrane trafficking is crucial for polar auxin transport, and suggest a role for vesicle transport in plant vasculature development.

We previously screened Arabidopsis mutants with aberrant cotyledon venation and isolated seven *van* (*vascular network defective*) mutants (Koizumi et al. 2000). Of these, we have identified the genes responsible for the *van3* and *van7* mutants. *VAN3* encodes an ARF-GAP protein that localizes primarily at the PM, and to a lesser extent at the *trans*-Golgi network/early endosome (TGN/EE), in developing organs; thus, VAN3 potentially regulates vesicle formation at the PM and TGN/EE (Koizumi et al. 2005, Sieburth et al. 2006, Naramoto et al. 2009, Naramoto et al. 2010). The *van7* mutant is a weak allele of the *gnom* mutant (Koizumi et al. 2000, Shevell et al. 2000, Kleine-Vehn et al. 2009). Our discovery of the involvement of VAN3 ARF-GAP and GNOM/VAN7 ARF-GEF in vein pattern formation strongly supports the tight coupling between vesicle transport and vascular development, particularly for procambium development.

In this study, we characterized the *van4* mutant that is crucial for vascular development to gain additional insights into vein pattern formation. The *VAN4* gene encoded a putative TRS120 protein, a Rab-GEF and/or tethering factor, which localizes at the TGN/EE. Phenotypic analysis showed that VAN4 regulates endocytic recycling that is involved in procambium development, subsequent vascular cell differentiation and normal cell growth. Our identification of VAN4 as a putative TRS120 provides evidence for the crucial importance of small GTPase-mediated vesicle trafficking in leaf vascular formation.

Results

Vascular tissue development in the *van4* mutant

Leaves of *van4* mutants have defects in vascular differentiation, but how *VAN4* regulates vascular development was not clear. Vascular cells differentiate from procambium cells, which arise in leaves from the ground meristem. To examine the steps of vascular tissue differentiation that are affected by the *VAN4* mutation, we introduced *pAthb8::GUS* (Baima et al. 1995) to the *van4* mutant as a marker of procambium cells. In wild-type cotyledons, *pAthb8::GUS* was continuously expressed along the mid-vein and the proximal and distal loops of lateral veins, which resulted in the contiguous procambium cell files developing venation (**Fig. 1A**). In *van4* mutant cotyledons, *pAthb8::GUS*-expressing cells occasionally formed discontinuous lateral loops (**Fig. 1B, C**; **Table 1**). Continuous loops of *pAthb8::GUS*-expressing cell files that did not develop vascular tracheary elements were also observed in *van4* mutants, and showed defects in later steps of vascular cell development (**Fig. 1C**). These results suggest that VAN4 is involved in early vascular patterning of the procambium network and later vascular cell differentiation, such as the development of tracheary elements from procambial cells.

To examine the relationship between VAN4 and auxin transport-mediated vascular pattern formation, we crossed

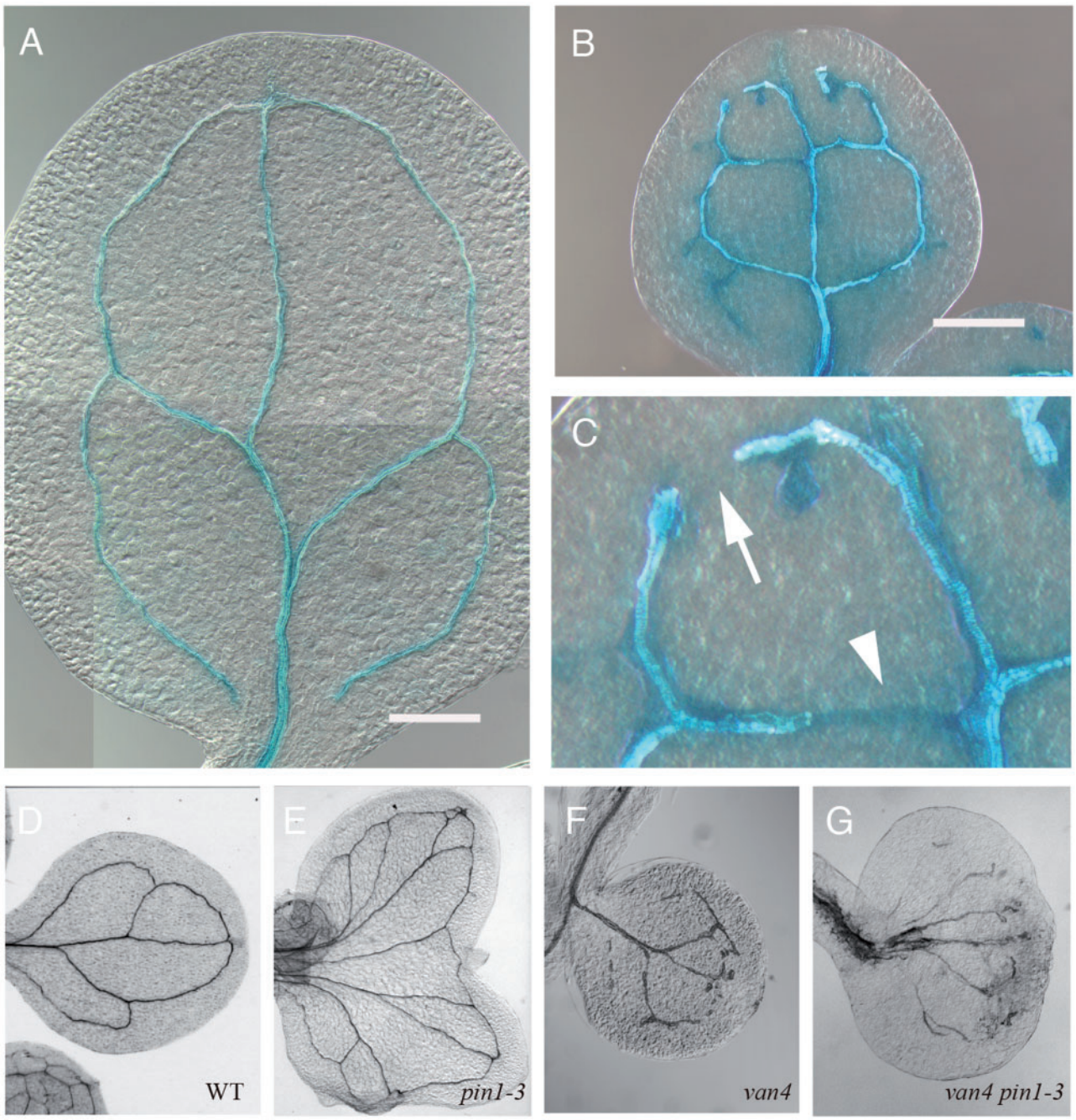

Fig. 1 Vascular phenotypes of *van4* mutants. (A–C) Expression patterns of *pAthb8::GUS* in wild-type cotyledons (A) and the *van4* mutant (B and C). (C) Close-up image of (B), which shows typical *van4* phenotypes. The arrow indicates the region that shows discontinuous procambium cells; the arrowhead indicates the region that shows continuous procambium cells that fail to differentiate into mature vascular cells, indicated by tracheary elements. (D–G) Vascular patterns in the cotyledons of wild-type (D), *pin1-3* (E), *van4* (F) and *van4 pin1*(G) seedlings. Scale bars = 200 μm (A–G).

the *van4* mutant with the *pin1-3* mutant, which is defective in polar auxin transport (Furutani et al. 2004), and analyzed the resulting venation patterns. The *van4* mutant had a discontinuous vascular network in cotyledons, but no significant effects on the overall vascular pattern architecture (**Fig. 1D, F**; **Table 2**). The *pin1-3* seedlings had fused cotyledons in which the mid-vein was occasionally furcated (**Fig. 1E**; **Table 2**) (Koizumi et al. 2005). Seedlings of the *van4 pin1-3* double mutant exhibited fused cotyledons in which discontinuous veins were formed, like those in *van4*, implying an additive effect of *VAN4* and *PIN1* mutations (**Fig. 1G**; **Table 2**). We also analyzed the effect of 1-*N*-naphthylphthalamic acid

PCP PLANT & CELL PHYSIOLOGY

Table 1 Characterization of the procambium network patterns in *van4* mutant cotyledons.

	No. of free ends	% of VIs
Wild type (31)	0.48 ± 0.63	0%
van4 (31)	1.61 ± 0.88[a]	6.45%

The vascular pattern is analyzed by observing the distribution pattern of *pAthb8*::*GUS*-expressing cells.
The numbers in parentheses represents the number of organs scored. % of VIs represents the percentage of cotyledons with vascular islands.
[a] Significantly different from the wild type.

Table 2 Cotyledon vascular pattern characters for various mutants

	No. of free ends	% of VIs	% of fused cotyledons
Wild type (22)	0.5 ± 0.67	0%	0%
van4 (28)	2.43 ± 1.45	10.7%	0%
pin1 (24)	0.42 ± 0.58	0%	62.5%
van4 pin1 (21)	2.71 ± 1.31[a]	14.3%	66.7%

Vascular pattern is analyzed by observing the distribution pattern of tracheary elements in cotyledons.
The numbers in parentheses represent the number of seedlings scored. % of VIs represents percentage of cotyledons having vascular islands.
[a] No significant difference from *van4* mutants

(NPA), an auxin transport inhibitor, on the vascular patterning in first-node leaves. NPA progressively enhanced the vascular differentiation, especially along the leaf margin, as the concentration of NPA was increased, and the marginal vascular tissues were connected to central vascular tissues in the wild-type (**Supplementary Fig. S1A–C**) (Mattsson et al., 1999). In *van4* mutant grown with NPA, vascularization was enhanced, which mimicked wild-type plants treated with NPA, but the vasculature often became disconnected at leaf margins, like those in *van4* (**Supplementary Fig. S1D–F**). Finally, we observed the PIN1–GFP localization during cotyledon vascular development. PIN1–GFP within the cells in the secondary vein was known to localize towards the primary veins in wild-type cells and these features were also observed in *van4* mutant cells (**Supplementary Fig. S2**). Dissection of cotyledons from embryos damaged the tissues, whose impact seemed to cause variations of PIN1–GFP signal intensity. Therefore, we cannot determine the amount of PIN1 protein at the PM in cotyledon veins; however, we could identify that the PIN1–GFP expression domain (PED) at the cotyledon margin in *van4* mutant is more fragile than in the wild type, which presumably leads to discontinuity of venation. These results suggest that VAN4 regulates venation patterning through primarily maintaining or establishing the PEDs rather than establishing the polar localization of PIN proteins.

Morphological analysis of *van4* mutants at the whole-plant level

To address further the role of VAN4 in plant development, we performed phenotypic analysis of the *van4* mutant at the whole-plant level. We analyzed the phenotypes of 14-day-old *van4* mutant seedlings. The *van4* mutant displayed smaller leaves and shorter primary roots than wild-type (*Ler*) seedlings (**Fig. 2A, B**), and these defects were lethal when the seedlings were approximately 4 weeks old. Serial observations revealed that the primary root length of *van4* was essentially the same as that of the wild type until 3 days after germination (DAG), whereas the slower growth of *van4* roots became obvious by 7 DAG. At 12 DAG, *van4* primary roots were five times shorter than those of the wild type, and *van4* developed more adventitious roots than the wild type (**Fig. 2B, C**). Next, we performed tissue culture experiments. We first induced adventitious root development from hypocotyls obtained from seedlings at 12 DAG. *Ler* hypocotyls actively produced adventitious roots, whereas the *van4* mutant hypocotyls produced fewer and shorter adventitious roots (**Fig. 2D, G**; **Supplementary Table S1**). We also induced adventitious shoots from hypocotyls and compared their growth. The induction of adventitious shoots was successful in wild-type hypocotyls, whereas the *van4* mutants did not develop any shoot-like structures, although they did develop greenish spots (**Fig. 2E, H**; **Supplementary Table S1**). Finally, we tested the induction of callus formation from hypocotyls. The *van4* calli grew more slowly than those of the wild type, which suggests that VAN4 function is necessary to maintain cell division (**Fig. 2F, I**; **Supplementary Table S1**). Together, these data indicate that VAN4 also functions in other developmental programs in addition to vascular development.

Positional cloning of the *VAN4* gene

VAN4 was previously mapped to the top of chromosome 5 (Koizumi et al. 2000). To clone *VAN4*, we generated a large mapping population from a cross between *van4* and wild-type Columbia. The population was scored for the mutant phenotype, and 671 mutant plants were selected and screened with polymorphic markers, which were designed based on the limited sequence data in the region mapped as the *VAN4* locus. Finally, *VAN4* was localized to the T5K6 BAC (bacterial artificial chromosome) clone, as illustrated in **Fig. 3A**. There were 14 genes in this region based on gene annotation. All 14 genes were completely sequenced in the *van4* background, and a C-to-T nucleotide transition mutation was found in the predicted coding sequence (CDS) of At5g11040 (**Fig. 3B**). To confirm that this gene is the causal gene of the *van4* mutant, the wild-type sequence that contains 2.2 kb upstream of the putative transcription start site and approximately 2.4 kb downstream of the putative transcription termination site was introduced into the *van4* mutant by *Agrobacterium*-mediated transformation. This region rescued the phenotype of the *van4* mutant, confirming that *VAN4* encodes At5g11040. We isolated the full-length *VAN4* cDNA by combination of 5′ RACE (rapid amplification of cDNA ends) and 3′ RACE, and defined the structure of the *VAN4* gene. The *VAN4* gene encoded a protein composed of 1,186 amino acids, and glutamine at

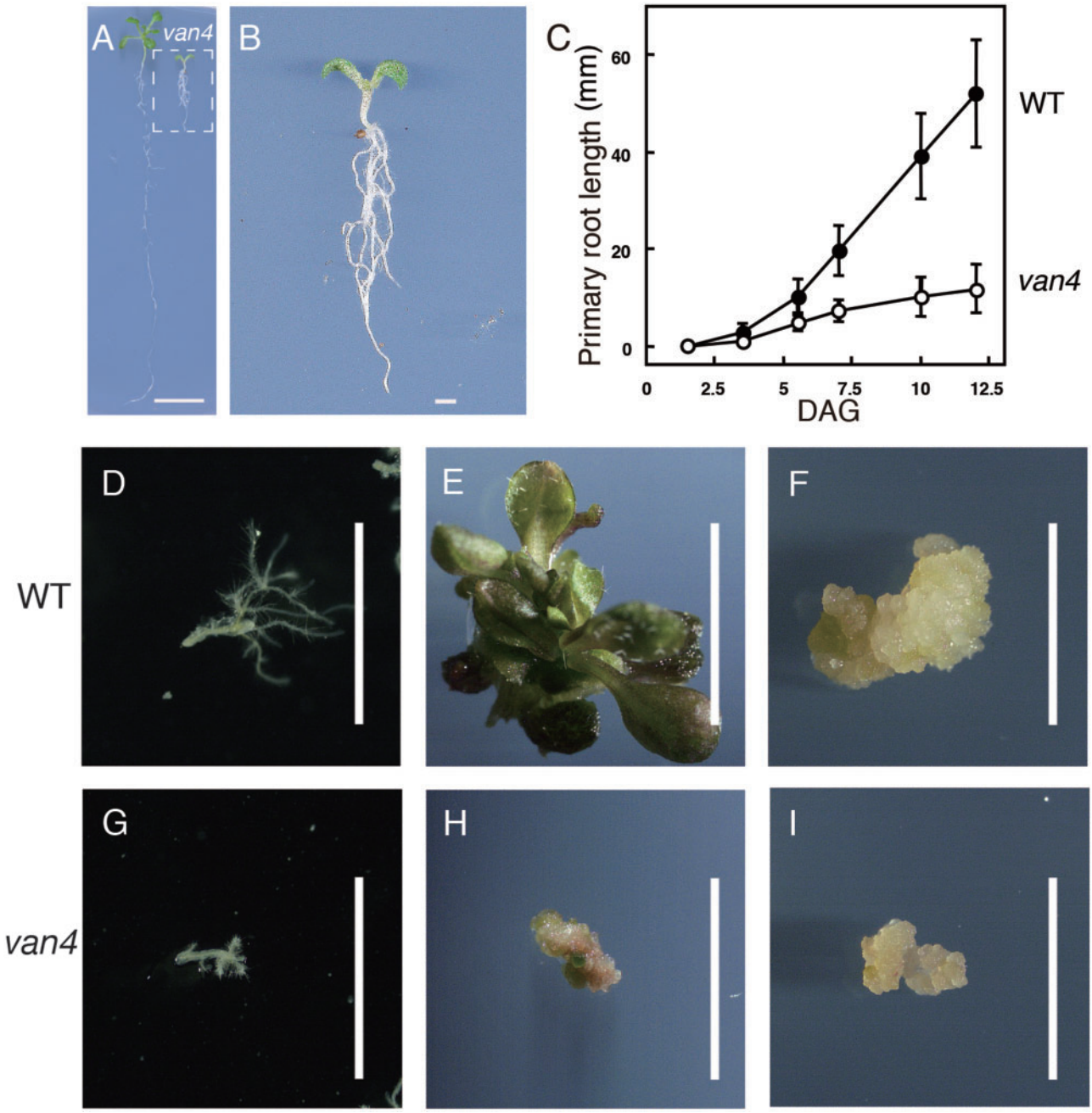

Fig. 2 Seedling phenotypes and tissue culture experiments of *van4* mutants. (A) Wild-type and *van4* mutant seedlings at 7 DAG. The wild type is shown on the left, and the *van4* mutant is indicated by a dashed box. (B) Close-up view of the dashed box in (A). (C) Measurement of primary root growth in wild-type and *van4* mutant seedlings. (D–I) Phenotypes of wild-type (D–F) and *van4* mutant (G–I) tissue cultures of root redifferentiation (D and G), shoot redifferentiation (E and H) and callus induction (F and I) from hypocotyl explants. Scale bars = (A) 1 cm, (B) 1 mm and (D–I) 5 mm.

codon 396 was changed to a stop codon in the *van4* mutant (**Fig. 3B**). At5g11040 was recently reported as a putative TRS120, a member of the TRAPPII complex that functions as a GEF for Ypt31/32 and/or a tethering factor (Jones et al. 2000, Morozova et al. 2006, Sacher et al. 2008). At5g11040 was shown to regulate exocytosis, the cell plate and cell polarity formation in Arabidopsis (Qi et al. 2011). We identified defects in cell division and venation in *van4* mutants. These similarities provided further evidence that *VAN4* encodes At5g11040.

VAN4 expression patterns in plants

We investigated *VAN4* expression patterns by performing RNA gel-blot analysis using digoxigenin-labeled antisense RNA probes for the cDNAs. RNA was isolated from roots, leaves,

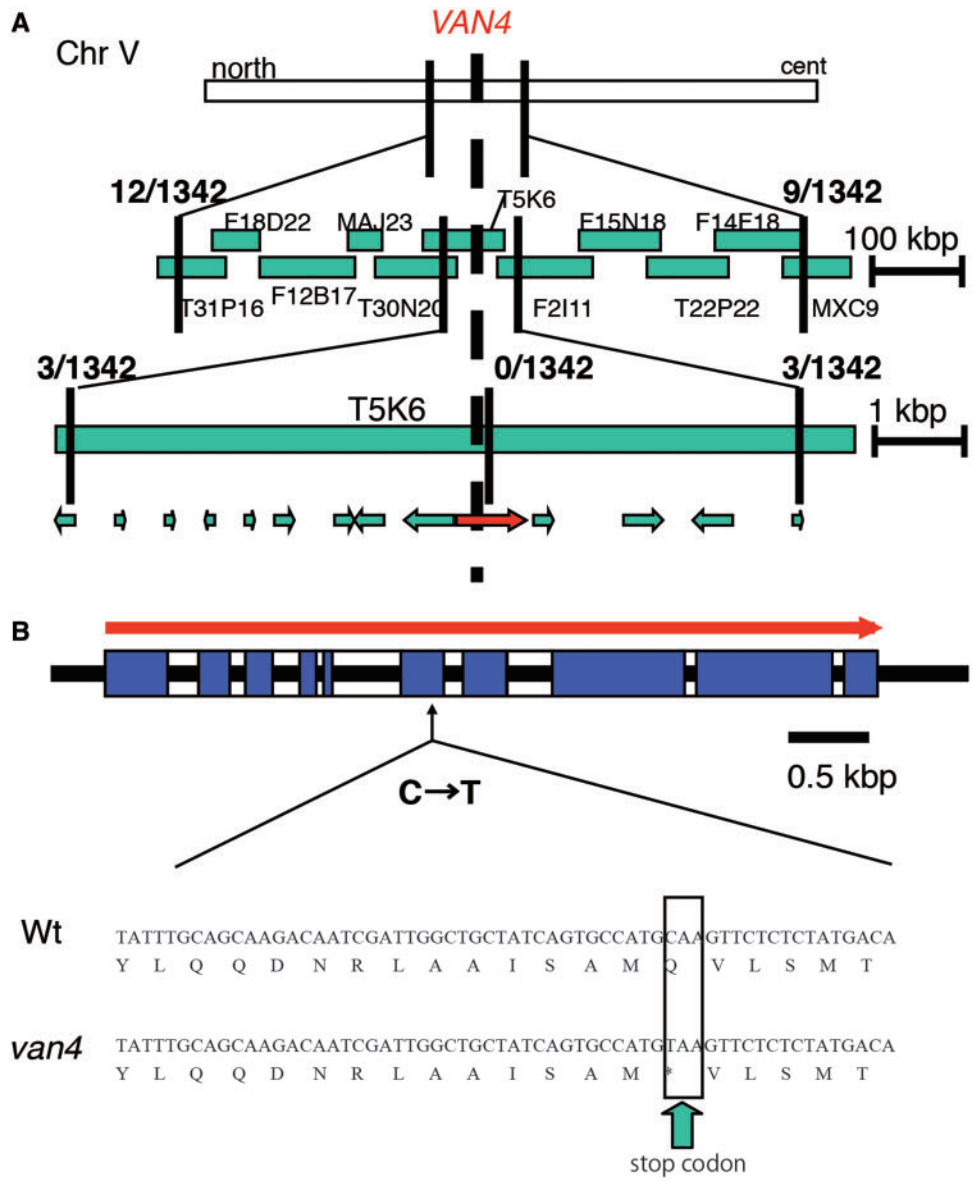

Fig. 3 Molecular cloning of *VAN4*. (A) Scheme showing the map-based cloning of *VAN4*. Open boxes indicate BAC clones around the *VAN4* mutation. Fractions for molecular markers indicate the number of meiotic events. Red arrows and green arrows show the *VAN4* gene and putative genes in this region, respectively. (B) Structure of *VAN4*. Blue boxes represent exons; white boxes represent introns. The nucleotide sequence at the *VAN4* mutation causes a nucleotide exchange from C to T.

stems and flowers. *VAN4* mRNA accumulated in all organs tested, which is consistent with previous data obtained by reverse transcription–PCR (RT–PCR) analyses (**Fig. 4**) (Qi et al. 2011). We identified differential accumulation of *VAN4* mRNA among different organs. *VAN4* mRNA accumulated to high levels in roots and flowers, which include meristematic cells (**Fig. 4**). These results suggest strong expression of *VAN4* in meristematic cells.

To examine further the expression pattern of *VAN4*, we produced transgenic plants harboring the β-glucuronidase (GUS) reporter gene fused to a 2.2 kbp upstream promoter region of *VAN4*. *pVAN4::GUS* expression was detected in flowers and roots. Strong expression was detected at root meristems and vascular cells in petals, stamens and roots (**Fig. 5A–D**). In pistils, *pVAN4::GUS* expression was detected particularly at vascular cells in the funiculus and ovules (**Fig. 5E, F**). Notably stronger expression was detected in immature vascular cells close to ovules, which implies a role for VAN4 in vascular development.

The *van4* mutant has a characteristic phenotype with respect to leaf vascular development. Therefore, we performed detailed analysis of *pVAN4::GUS* expression during venation development. We initially analyzed *pVAN4::GUS* expression in torpedo stage embryos, when the differentiation of

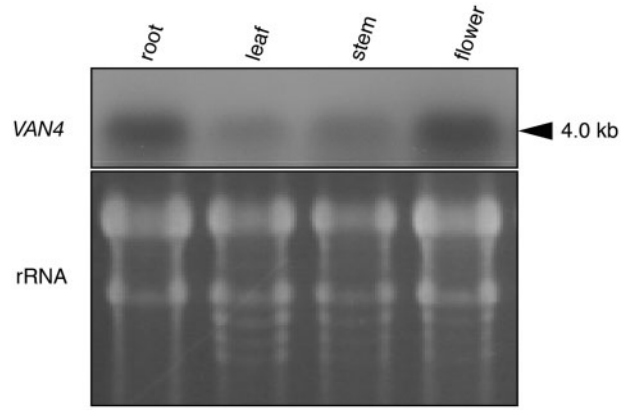

Fig. 4 RNA gel-blot analysis for tissue-specific expression of *VAN4*. Total RNA was isolated from roots, leaves, stems and flowers. *VAN4* cDNA was used to probe the RNA gel blot, and the corresponding ethidium bromide-stained rRNA is shown as a loading control.

procambium cells in cotyledons starts. *pVAN4::GUS* expression was ubiquitous throughout the torpedo embryo, and the expression level was largely uniform among the tissues (**Fig. 5G, H**). Next, we analyzed *pVAN4::GUS* expression in cotyledons of seedlings at 7 DAG, when procambium cells differentiate into vascular cells, including xylem cells, and found that *pVAN4::GUS* expression was confined to the veins (**Fig. 5I**), with strong expression in procambium cells (**Fig. 5J**). These expression patterns are in good agreement with the venation defects of *van4* mutants.

VAN4 is a peripheral membrane protein

Subcellular localization analysis of VAN4/TRS120 has not been reported. To examine the intracellular localization of VAN4, we analyzed the association of VAN4 with plant membranes. For this experiment, we produced a plasmid in which the *VAN4* CDS containing the 2.2 kb promoter and the 2.4 kb 3′ untranslated region (UTR) was fused with the C-terminal 3× myc tag. This plasmid complemented the *van4* mutants when introduced into *van4* by *Agrobacterium*-mediated transformation, indicating that the VAN4-3×myc fusion protein is fully functional. We prepared microsomal membrane and soluble protein fractions from the *pVAN4::VAN4-3×myc* transgenic plants, and examined the presence of VAN4 with an anti-myc antibody. The VAN4 protein was detected in both the membrane and the soluble fraction, but it was more enriched in the membrane fraction (**Fig. 6A**). The membrane association was sensitive to urea, Na_2CO_3, Triton X-100 and CHAPs, whereas it was resistant to NaCl (**Fig. 6A**). These results indicate that VAN4 is not an integral membrane protein, but a peripheral membrane protein that associates with plant membranes via non-electrostatic interactions.

Subcellular localization of VAN4

To gain insights into the intracellular site of VAN4 activity, we examined localization of VAN4 proteins using anti-myc

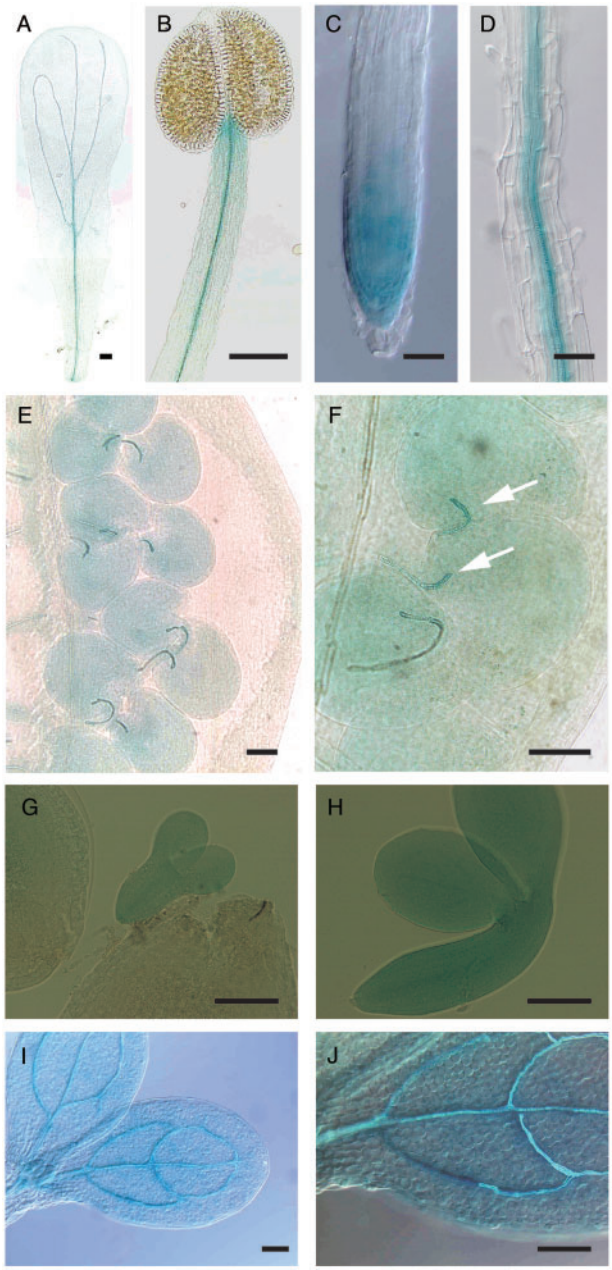

Fig. 5 Expression patterns of *proVAN4::GUS* in Arabidopsis. (A–F) *proVAN4::GUS* expression in petals (A), stamens (B), root meristem (C), primary root (D) and ovules (E and F). (G–I) *proVAN4::GUS* expression in early torpedo stage embryos (G), late torpedo stage embryos (H) and cotyledons of seedlings at 7 DAG (I). (J) Close-up view of the 7 DAG seedling cotyledons shown in (I). Arrows indicate strong expression of *proVAN4::GUS* at immature vascular cells that are close to ovules. Scale bars = (A–F and I–J) 100 μm and (G and H) 30 μm.

antibody in the roots of transgenic Arabidopsis plants expressing *VAN4-3×myc* under the control of the *VAN4* promoter. We failed to detect reliable signals under normal conditions. However, some signals were detected in the presence of BFA, an ARF-GEF inhibitor. In Arabidopsis, BFA treatment induces the aggregation of endosomes into so-called BFA bodies

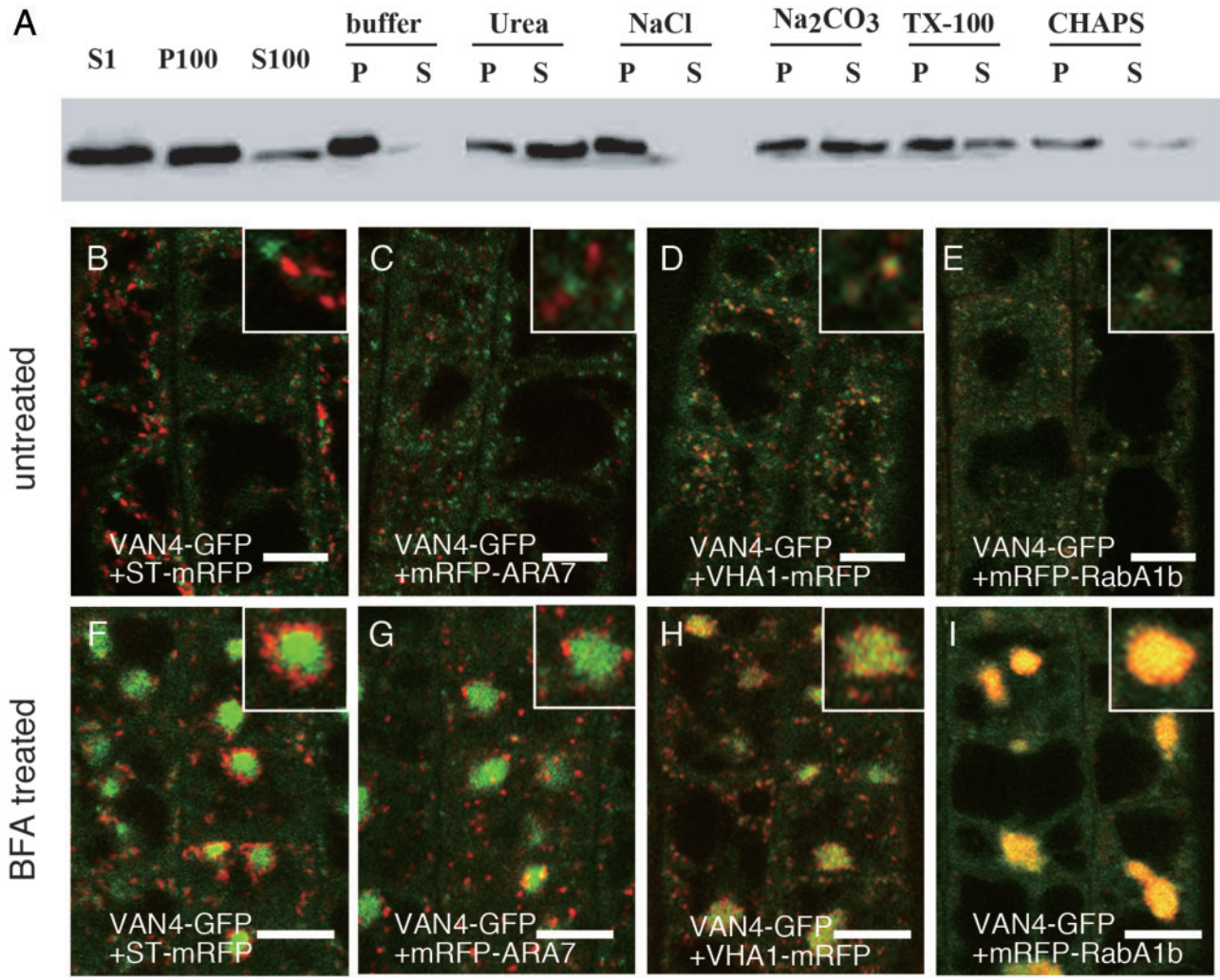

Fig. 6 Subcellular localization analysis of VAN4. (A) Membrane binding assay of VAN4-3×myc. Extracts of transgenic *van4* mutants expressing the *VAN4-3×myc* construct were centrifuged at 1,000×*g* to yield a total cell extract (S1). The S1 fraction was centrifuged at 100,000×*g* to yield soluble (S100) and membrane (P100) fractions. The P100 fraction was incubated on ice in a buffer containing either urea, salt, alkali (Na_2CO3), Triton X-100 or CHAPS, and subsequently centrifuged at 100,000×*g* to yield soluble (S) and membrane (P) fractions. These fractions were analyzed by immunoblotting with anti-myc antibody. (B–I) Confocal images of VAN4–GFP (green) and RFP-tagged intracellular markers (red) in root cells. (B–E) Merged images of VAN4–GFP with ST–mRFP (B), mRFP–Ara7 (C), VHA1–mRFP (D) and mRFP–RabA1b (E) in untreated root cells. (F–I) Merged images of VAN4–GFP with ST–mRFP (F), mRFP–Ara7 (G), VHA1–mRFP (H) and mRFP–RabA1b (I) in BFA-treated root cells.

surrounded by Golgi bodies (Geldner et al. 2003). VAN4-3×myc localized at the core of BFA bodies, and the Golgi marker ST–GFP (Wee et al. 1998) distinctly surrounded the BFA bodies. These results suggest that VAN4 proteins are localized in endosomes (**Supplementary Fig. S3**).

The failure of immunostaining of VAN4-3×myc under normal untreated conditions may result from instability of VAN4-3×myc during fixation. To overcome this problem, we established transgenic *van4* mutants complemented by the expression of *pVAN4::VAN4-GFP*. Functional *pVAN4::VAN4-GFP* lines were crossed with monomeric red fluorescent protein (mRFP)-tagged organelle marker lines, and we observed the root cells. Dot-like signals of VAN4–GFP were not significantly localized with the Golgi marker ST–mRFP (Wee et al. 1998) or the pre-vacuolar compartment/multivesicular body (PVC/MVB) marker mRFP–Ara7 (**Fig. 6B, C**; **Supplementary Fig. S4**) (Ueda et al. 2001). In contrast, significant co-localization between VAN4–GFP and the TGN/EE marker vacuolar H^+-ATPase subunit 1 (VHA1)–mRFP or mRFP–RabA1b was observed (**Fig. 6D, E**; **Supplementary Fig. S4**) (Dettmer et al. 2006, Asaoka et al. 2012). We also analyzed the effects of BFA on the localization of VAN4–GFP. Similar to the case with VAN4-3×myc, BFA caused aggregation of VAN4–GFP surrounded by the ST–mRFP-labeled organelles (**Fig. 6F**). No significant co-localization was observed between VAN4–GFP and ST–mRFP (**Fig. 6F**), or between VAN4–GFP and mRFP–Ara7 (**Fig. 6G**). VAN4–GFP co-localized with VHA1–mRFP (**Fig. 6H**) and with mRFP–RabA1b at the core of BFA bodies (**Fig. 6I**).

Furthermore, mRFP–RabA1b almost completely co-localized with VAN4–GFP at the BFA body, implying their close relationships. These data indicate that VAN4 acts at TGN/EE compartments.

Defective exocytosis of PIN proteins in *van4* mutants

Based on the subcellular localization, it is conceivable that VAN4 may regulate membrane trafficking in the translocation of cargo to the PM or other cellular compartments. PIN proteins undergo constitutive clathrin-mediated endocytosis and subsequent recycling to PMs; thus, they are good markers to visualize protein internalization and recycling (Dhonukshe et al. 2007, Robert et al. 2010). Since analyzing the intracellular function of VAN4 by using leaf vascular cells was technically difficult, we used *van4* root cells to analyze endocytic recycling of PIN proteins. First, we performed immunolocalization of PIN1 and PIN2 under normal conditions. In wild-type cells, PIN1 localized to the basal (rootward) sides of PMs in vascular cells, whereas PIN2 localized apically (shootward) and basally at the PMs in epidermal and cortical cells, respectively (**Fig. 7A**). In *van4* roots, the polar localization of PIN proteins is largely normal, which fits with our phenotypic analysis of *pin1 van4* double mutants. However, increased internalization of PIN proteins was observed in *van4* roots (**Fig. 7C, E**). We also applied BFA to *van4* root cells to examine whether VAN4 was required for the cycling of PIN proteins. BFA predominantly inhibits the exocytic pathway rather than the endocytic pathway, so that the ratio between exocytosis and endocytosis is perturbed, and endocytic materials accumulate in the cell (Geldner et al. 2001, Dhonukshe et al. 2007). Consistent with previous studies, treatment of wild-type roots with BFA led to PIN1 and PIN2 accumulation in typically two or three large endosomal aggregations (**Fig. 7B**). In contrast, BFA treatment of *van4* mutants resulted in PIN1 and PIN2 localization in more numerous and larger endosomal aggregates in each cell (**Fig. 7D, F**). We also analyzed the protein levels of PIN1 at PMs in *van4* mutants. We used PIN1–GFP lines instead of PIN1 antibody because immune detection often causes the variation of signal intensity. Signal intensity of PIN1–GFP at PMs in *van4* mutants was significantly lower than that of the wild type (**Supplementary Fig. S5**). Altogether, these results suggest that VAN4 is required for normal cycling of PIN proteins, possibly in the delivery of exocytic vesicles to the PM.

Discussion

VAN4 encodes a putative TRS120 protein localized at the TGN/EE

The vesicle transport system promotes the formation of a continuous vascular network by regulating endocytic recycling of PIN proteins. Together with the results of other groups, we reported that VAN3/SFC, ARF-GAP and VAN7/GNOM ARF-GEF regulate the venation pattern by controlling the activity of the ARF GTPase involved in vesicle formation, cargo loading and vesicle budding (Koizumi et al. 2000, Koizumi et al. 2005, Sieburth et al. 2006, Naramoto et al. 2009, Naramoto et al. 2010). Here, we showed that *VAN4*, which is required for venation development and cellular growth, encoded a putative TRS120. TRS120 is a subunit of the TRAPPII complex protein that functions as a GEF for Rab GTPase and/or a tethering factor (Jones et al. 2000, Morozova et al. 2006, Sacher et al. 2008). Rab-GEFs are activators of Rab proteins, which convert Rab-GDP into the active Rab-GTP form. The conversion of Rab-GDP to Rab-GTP mediates tethering/docking of vesicles to specific target membranes (Zerial and McBride 2001, Cai et al. 2007). Our finding that *VAN4* encodes a putative TRS120 provides further support for the importance of vesicle transport in vein pattern formation.

The TRAPPII complex localizes at the late Golgi and endosomes in yeasts, whereas it localizes at the early Golgi in animals (Cai et al. 2005, Yamasaki et al. 2009). This difference may suggest distinct subcellular roles for TRAPPII in different kingdoms. In plants, the subcellular localization of TRS120 has not yet been reported. TRS130–YFP (yellow fluorescent protein), a fusion construct of another component of the TRAPPII complex, was observed to localize at the TGN when it was overexpressed (Qi et al. 2011). However, this result was not conclusive, because co-localization analysis of TRS130 with markers for the Golgi apparatus and the PVC/MVB has not been tested (Qi et al. 2011). These facts raise questions about the subcellular localization of the TRAPPII complex in plants. In this study, we performed detailed subcellular localization analysis of putative AtTRS120/VAN4. We demonstrated that functional VAN4–GFP co-localized with the TGN/EE markers VHA1–mRFP and mRFP–RabA1b, but not with Golgi and PVC/MVB markers (**Fig. 6B–I**). These results strongly suggest that VAN4 localizes at the TGN/EE.

In yeast, TRAPPII is suggested to act as a GEF for Rab proteins, particularly Ypt1 and Ypt31/32 (Jones et al. 2000, Morozova et al. 2006, Cai et al. 2008). In Arabidopsis, RabD and RabA are homologs of Ypt1 and Ypt31/32, respectively; thus, they could be substrates of AtTRAPPII complex proteins (Qi and Zheng 2011). We found significant co-localization of VAN4 with RabA1b, suggesting that VAN4 may be an activator of RabA1 proteins. This idea is supported by the recent report that the phenotype of *attrs130* mutants was suppressed by expression of a constitutively active form of RabA1c but not that of RabD2a (Qi and Zheng 2011, Qi et al. 2011). A role for RabA1b in exocytosis is also suggested (Feraru et al. 2012). We identified exocytic defects of PIN proteins in *van4* mutants. Although these results suggest a role for the AtTRAPPII complex as a GEF for RabA1 proteins but not for RabD, further analysis, including measurement of the GEF activity of TRAPPII, will be necessary to elucidate its molecular function. We are currently establishing systems for measuring the GEF activity of the AtTRAPPII complex.

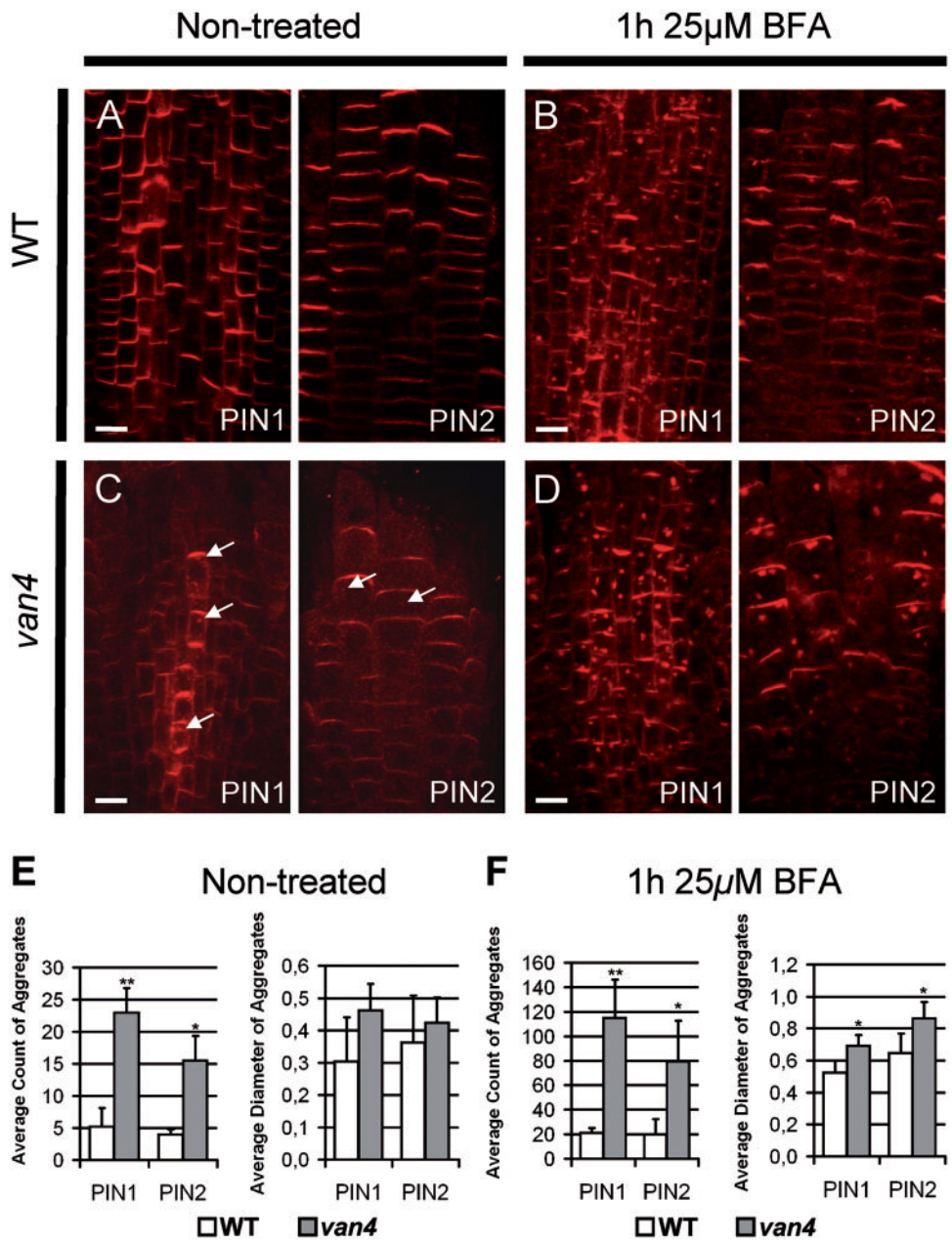

Fig. 7 Subcellular localization analysis of PIN1 and PIN2 in *van4* mutants. (A–D) Immunolocalization of PIN1 and PIN2 in wild-type and *VAN4* seedlings that were untreated (A and C) or treated with 25 μM BFA for 1 h (B and D). Arrows indicate internalized PIN proteins. (E and F) Statistical analysis of PIN1 and PIN2 intracellular aggregate numbers and diameters in wild-type and *VAN4* seedlings that were untreated (E) or treated with 25 μM BFA for 1 h (F). Scale bars = (A–F) 10 μm. (E and F) Error bars in graphs represent the SD deviation; $^{*}P < 0.05$; $^{**}P < 0.01$.

VAN4 regulates multiple roles in plant development

The *van4* mutant is isolated by a defect in the venation pattern. Besides the venation defects, we also identified defects in root development (**Fig. 2**). In tissue cultures, both root and shoot differentiation was severely inhibited in *van4* mutants. The growth of callus was much slower in *van4* mutants than in the wild type (**Fig. 2**; **Supplementary Table S1**). These results indicate that VAN4 is also involved in organ development and proliferation. We examined the *VAN4* expression pattern by RNA gel-blot analysis and GUS staining of *pVAN4::GUS* seedlings, which indicated that *VAN4* expression was high in meristematic cells of shoots, roots and leaf vascular cells (**Fig. 5**). These expression patterns are consistent with the observed phenotype of *van4* mutants (**Fig. 2**). Independent from our research, Qi and co-workers recently identified cell wall stubs, aberrant root meristem structures and abnormal cell shapes in *attrs120* mutants (Qi et al. 2011). Therefore, defects in shoot,

root and callus growth in *van4* mutants may be attributed to aberrant cell division, including slower cytokinesis and immature cell plate formation. In contrast, the inhibition of tracheary element differentiation from procambium cells in *van4* mutants cannot be explained by defects in cell division. Therefore, VAN4 is predicted to be more widely involved in cell growth and development.

Role of VAN4 in exocytosis

To elucidate the intracellular function of VAN4 proteins, we analyzed the subcellular localization of PIN proteins as cargo of vesicle trafficking pathways. Although the *VAN4* mutation did not affect the polar localization of PIN proteins, it caused aberrant intracellular accumulation of PIN proteins, which suggested that VAN4 functions in the exocytic pathway. This result is further supported by pharmacological experiments with BFA, a widely used inhibitor of the recycling pathway of PM cargoes, which induces the aggregation of endosomes into the BFA body. The size and number of BFA bodies are determined by the balance between endocytic and exocytic pathways, and larger and more numerous BFA bodies indicate stimulated endocytosis or inhibited exocytosis of PM cargoes, including PIN proteins (Geldner et al. 2003, Dhonukshe et al. 2007, Robert et al. 2010). In BFA-treated *van4* root cells, larger and more numerous endosomal aggregations of PIN1 and PIN2 were observed (**Fig. 7**). A previous study on AtTRS120 indicated its involvement in exocytosis (Qi et al. 2011). RabA1bS24N, a dominant-negative form of RabA1b, induced bigger BFA bodies and exocytic defects of PIN1 and PIN2 (Feraru et al. 2012). These results suggest that VAN4/TRS120 plays an essential role in exocytosis.

Qi and co-workers detected polarity defects and abnormal intracellular aggregation of PIN2–GFP in *attrs120* mutants, whereas PIN1–GFP localized normally. Based on these data, the role of TRS120 in selective exocytosis that transports PIN2 but not PIN1 was proposed (Qi et al. 2011). However, we detected endocytic recycling defects of both PIN1 and PIN2 in *van4* mutants, without affecting their polar localization (**Fig. 7**). These differences may be attributed to different experimental methods. We used specific antibodies for PIN1 and PIN2 instead of GFP-tagged PIN proteins. Immunolocalization analyses of endogenous PIN1 and PIN2 with these antibodies have been conducted rigorously, and their reliability has been confirmed. Further analysis is necessary to elucidate whether VAN4/TRS120 regulates the general exocytic pathway or the PIN2-specific exocytic pathway, although the general expression of *VAN4/TRS120* supports its general function in exocytosis.

Involvement of the *VAN4* gene in vascular development

Detailed phenotypic analysis of the *van4* mutant using *pAthb8::GUS* transgenic plants revealed that the discontinuous venation is caused by discontinuous formation of procambium cells and retarded differentiation of vascular cells, such as tracheary elements in the lateral vein (**Fig. 1B, C**). Consistent with these phenotypes, *pVAN4::GUS* is strongly expressed in procambium cells (**Fig. 5I, J**), whereas *VAN4* is expressed ubiquitously in cotyledons of torpedo stage embryos when procambium cells start to differentiate (**Fig. 5G, H**). Vascular cell differentiation is categorized into at least two steps, i.e. procambium cell differentiation and subsequent differentiation into vascular cells, such as xylem and phloem. These results strongly suggest that VAN4 plays crucial roles in vascular cell differentiation at both steps.

VAN4/TRS120 is suggested to function in exocytosis. How does VAN4-mediated vesicle transport regulate continuous venation? There is an auxin signal flow canalization hypothesis for explaining vein pattern formation (Sachs 1981, Sachs 1989, Sachs 1991). According to this hypothesis, directed auxin flow, which is determined by the polar localization of PIN proteins, determines vein pattern. The polar localization of PIN proteins is regulated by continuous endocytic recycling between the PM and endosomes (Kitakura et al. 2011, Kleine-Vehn et al. 2011). To investigate whether VAN4 regulates procambium cell continuity through PIN proteins, we performed a combination of genetic, pharmacological and cell biological analyses of PIN and VAN4. Although phenotypic analysis of *pin1-3 van4* double mutants and NPA treatment experiments favored the independent function of these genes (**Fig. 1D–G**; **Supplementary Fig. S1**), and the polar localization of PIN1 in *van4* mutants was largely normal (**Fig. 7**; **Supplementary Fig. S2**), our experiments revealed defects in endocytic recycling of PIN proteins in *van4* root cells (**Fig. 7**). Furthermore, we also detected defects in maintaining or establishing the continuous PED in *van4* cotyledon venations (**Supplementary Fig. S2**). Considering the findings of a lower amount of PIN1 proteins at PMs in *van4* mutant root cells (**Supplementary Fig. S5**), we may speculate that a reduced amount of PIN proteins at PMs, caused by retarded recycling of PIN1 in *van4* mutants, somehow leads to a failure to maintain or establish the coordinated PED, resulting in discontinuous formation of procambium cells.

The *van4* mutant also exhibits a defect in terminal differentiation into tracheary elements. Tracheary elements develop elaborately patterned secondary cell walls. The process of secondary cell wall development during tracheary element formation involves new synthesis and transport of various cell wall-related enzymes to the PM/extracellular space. Therefore, we speculate that the retarded exocytosis of cell wall-related enzymes in the *van4* mutant leads to morphological defects of tracheary element differentiation.

Our mutant screening for altered venation patterns identified mutations whose causal genes encode vesicle transport-related proteins, such as ARF-GAP and ARF-GEF (Koizumi et al. 2000, Koizumi et al. 2005, Naramoto et al. 2009, Naramoto et al. 2010). In this paper, we revealed that *VAN4* encodes a putative GEF for Rab GTPase, which functions in procambium and subsequent vascular cell differentiation. Although this result suggested a role for Rab GTPase in venation development, how Rab

GTPase controls venation development is still unknown. Efforts are underway to identify the cargoes responsible for venation discontinuity in *van4* mutants, which will cast new light onto understanding the relationship between the Rab-mediated membrane transport system and leaf vascular development.

Materials and Methods

Plant growth conditions

Surface-sterilized seeds were plated on growth medium containing Murashige and Skoog basal salts, 1.0% (w/v) sucrose, 0.05% (w/v) MES (pH 5.7) and 0.8% (w/v) Bact Agar (Becton-Dickinson). Seeds were then transferred to a growth room at 22°C under continuous white light (20–50 μmol m^{-2} s^{-1}).

Positional cloning of *VAN4*

van4 (L*er*) was crossed to Col to generate a large mapping population of F_2 seedlings. Medium-grown F_2 seedlings were scored for the mutant cotyledon vascular patterning phenotype. DNA was isolated from a cotyledon and scored for recombinants. Novel polymorphic markers were developed by searching the databases of TAIR and Cereon Genomics. Using these markers, the position of the *VAN4* locus was determined in the 80 kb region in the T5K6 BAC clone including 14 putative genes (Arabidopsis Genome Initiative). These genes were PCR amplified from L*er* and *van4* as template, and completely sequenced by performing the cycle sequence reactions with a BigDye Terminator Cycle Sequencing Kit and subsequent sequence analysis of their sequences using the ABI PRISM 310 Genetic Analyzer. Among these putative genes, only *At5g11040* contained a point mutation in a putative exon. For complementation of the *van4* mutation, a 9.4 kb *Bgl*II–*Bgl*II genomic fragment that included the 2.2 kb upstream region of this gene and 2.4 kb downstream region was cloned into the binary vector pCAMBIA 1300 (CAMBIA). The clone was electroporated into *Agrobacterium tumefaciens* strain GV3101::pMP90 and transformed into plants carrying the heterozygous *van4* mutation (*van4*/*VAN4*) using the floral dip method.

Plasmid construction and histochemical staining for GUS

For construction of the *pVAN4::GUS* plasmid, the 2 kb upstream sequence of the *VAN4* transcriptional start site was amplified from Arabidopsis ecotype Columbia genomic DNA by PCR with gene-specific primer sets. They were subcloned into pENTR/D/TOPO vector (Invitrogen), and then integrated into the pBGGUS binary vectors (Kubo et al. 2005). The resulting plasmids were transformed into Arabidopsis ecotype Columbia by the floral dip method. Histochemical GUS staining was performed with seedlings of the F_2 generation. Samples were fixed in 90% (v/v) acetone for >45 min at −20°C. After washing in 100 mM sodium phosphate buffer pH 7.2 at least three times, they were immersed in a reaction mixture containing 1 mM 5-bromo-4-chloro-3-indolyl glucuronide, 0.5 mM potassium ferricyanide and 0.5 mM potassium ferrocyanide in 100 mM sodium phosphate buffer pH 7.2 and incubated at 37°C for 2 h in the dark. After the reaction, samples were mounted with a mixture of chloral hydrate, glycerol and water, and observed under a light microscope equipped with Nomarski optics.

Establishment of *VAN4-3×myc/GFP* transgenic lines

$3\times[(Gly)_3Ser]$-3×myc and -GFP encoded fragments were amplified by PCR from pDual GC (Stratagene) and pGWB1 plasmids as templates. The *VAN4-3×myc/GFP* reporter construct was obtained by the triple-template-PCR (TT-PCR) method (Tian et al. 2004) from both $3\times[(Gly)_3Ser]$-3×myc or -GFP encoded fragments and the Columbia genomic DNA fragment as templates. Inserting the $3\times[(Gly)_3Ser]$ linker-tagged *3×myc* or *GFP* open reading frame (ORF) in frame with the 3′ end of the *VAN4* ORF leads to a VAN4-3×myc/GFP translational fusion that complemented the mutant phenotype. All the PCR-amplified region of the construct was completely sequenced. At least five independent lines were investigated.

Fractionation of VAN4-3×myc

Two-week-old Arabidopsis seedlings were ground in GR buffer [50 mM HEPES-KOH pH 8.0, 330 mM sorbitol, 2 mM EDTA, 100 μM phenylmethylsulfonyl fluoride (PMSF), 10 μg ml^{-1} leupeptin and 10 μg ml^{-1} pepstain A], filtered through a 70 μm lattice Cell Strainer (Becton Dickinson) and centrifuged at 1,000×*g* for 5 min to remove cell debris. Supernatant (S1) was centrifuged at 100,000×*g* for 1 h to separate the crude membrane fraction (P100) from the cytosol (S100). For solubilization, the P100 fraction was resuspended in GR buffer plus 1 M NaCl, 2 M urea, 0.1 M Na_2CO_3, 1% Triton X-100, 1% CHAPS or 1 % SDS and incubated on ice for 1 h. Samples were then centrifuged at 100,000×*g* for 1 h to separate soluble from insoluble fractions and subjected to immunoblotting analysis with 9E-10 anti-cmyc antibody (SantaCruz). Anti-cmyc was diluted to 1 : 500 in the analysis of VAN4-3×myc.

Whole-mount immunolocalization

The procedure for whole-mount preparations was slightly modified from Paciorek et al. (2006). The 3- to 6-day-old Arabidopsis seedlings were fixed in 4% paraformaldehyde in MTSB pH 7.0 (50 mM PIPES, 5 mM EGTA, 5 mM $MgSO_4$ adjusted with KOH) for 1 h. Samples were washed with 0.1% Triton in MTSB (5× 5 min). Cell wall was digested with 1% driselase (Sigma-Aldrich) in MTSB for 45 min, and samples were washed with 0.1% Triton in MTSB (5× 5 min). The plasma membrane was permeablized with 10% dimethylsulfoxide (DMSO)/3% NP-40 in MTSB for 1 h. After another wash in 0.1% Triton in MTSB (5× 5 min), seedlings were pre-incubated in 2% bovoine serum albumin (BSA) in MTSB for blocking the unspecific interactions and incubated with the primary antibody in 3 % BSA in MTSB

(overnight, 37 °C). After extensive washing with 0.1 % Triton in MTSB (5 × 5 min), the seedlings were incubated with a secondary antibody in 3% BSA in MTSB (3 h, 37°C). In double labeling experiments, the antibodies were concomitantly incubated for the reaction of both primary and secondary antibodies. Finally, samples were washed with 0.1% Triton in MTSB (5× 5 min) and deionized water (5× 5 min) and transferred into Slowfade antifade mounting medium (Invitrogen). Primary antibodies were used at the following concentrations: anti PIN1 antibody and its dilution is 1 : 1,000; (Gälweiler et al. 1998), 1 : 400; 9E-10 anti-cmyc (SantaCruz), 1 : 250; and anti-GFP (Invitrogen), 1 : 200. Fluorochrome-conjugated secondary antibodies were used at the following concentrations: anti-rabbit–Alexa Fluor 488 (Invtirogen), 1 : 200; anti-rabiit-Cy3 (Sigma-Aldrich), 1 : 6 00; and anti-mouse-Alexa Fluor 568 (Invtirogen), 1 : 200.

Confocal laser scanning microscopy

Fluorescence signals were detected with either an Olympus FV1200 or a Zeiss LSM710 confocal microscope with a ×63 water immersion objective lens. For measurement of co-localization events, the distance between the centroids of two labeled objects was calculated by MetaMorph Software. When the distance was lower than the resolution limit of the objective used, it was recognized as a co-localization event. Images from at least three independent roots were subjected to analysis. For measuring the signal intensity of PIN1–GFP in primary roots, we measured the pixel gray value that encompasses the whole diameter of the PIN1-GFP signal in the stele by ImageJ software and averaged it for five Z-stack maximal projections. Each image was processed using Adobe Photoshop CS (Adobe Systems Inc.).

Supplementary data

Supplementary data are available at PCP online.

Funding

This work was supported by the Japanese Society for the Promotion of Science [JSPS; 30612022 to S.N. and 23227001 to H.F.]; the Ministry of Education, Culture, Sports, Science and Technology in Japan [NC-CARP project (to S.N. and H.F.)]; ERC Independent Research grant [ERC-2011-StG-20101109-PSDP to J.F.]; the European Social Fund and the state budget of the Czech Republic [the project 'Employment of Newly Graduated Doctors of Science for Scientific Excellence' (CZ.1.07/2.3.00/30.0009) (to T.N.)]; the Czech Science Foundation (GACR) [project 13-40637S (to J.F.)].

Acknowledgments

We gratefully acknowledge Simona Baima, Akihiko Nakano and Karin Schumacher for providing published materials, Munetaka Sugiyama for helpful discussion, and Rebecca Horn for help in preparing the manuscript.

Disclosures

The authors have no conflicts of interest to declare.

References

Aloni, R. (2001) Foliar and axial aspects of vascular differentiation: hypotheses and evidence. *J. Plant Growth Regul.* 20: 22–34.

Asaoka, R., Uemura, T., Ito, J., Fujimoto, M., Ito, E., Ueda, T. et al. (2012) Arabidopsis RABA1 GTPases are involved in transport between the trans-Golgi network and the plasma membrane, and are required for salinity stress tolerance. *Plant J.* 73: 240–249.

Baima, S., Nobili, F., Sessa, G., Lucchetti, S., Ruberti, I. and Morelli, G. (1995) The expression of the Athb-8 homeobox gene is restricted to provascular cells in Arabidopsis thaliana. *Development* 121: 4171–4182.

Berleth, T., Mattsson, J. and Hardtke, C.S. (2000) Vascular continuity and auxin signals. *Trends Plant Sci.* 5: 387–393.

Cai, H., Reinisch, K. and Ferro-Novick, S. (2007) Coats, tethers, Rabs, and SNAREs work together to mediate the intracellular destination of a transport vesicle. *Dev. Cell* 12: 671–682.

Cai, H., Zhang, Y., Pypaert, M., Walker, L. and Ferro-Novick, S. (2005) Mutants in trs120 disrupt traffic from the early endosome to the late Golgi. *J. Cell Biol.* 171: 823–833.

Cai, Y., Chin, H.F., Lazarova, D., Menon, S., Fu, C., Cai, H. et al. (2008) The structural basis for activation of the Rab Ypt1p by the TRAPP membrane-tethering complexes. *Cell* 133: 1202–1213.

Dettmer, J., Hong-Hermesdorf, A., Stierhof, Y. and Schumacher, K. (2006) Vacuolar H+-ATPase activity is required for endocytic and secretory trafficking in Arabidopsis. *Plant Cell* 18: 715–730.

Dhonukshe, P., Aniento, F., Hwang, I., Robinson, D., Mravec, J., Stierhof, Y. et al. (2007) Clathrin-mediated constitutive endocytosis of PIN auxin efflux carriers in Arabidopsis. *Curr. Biol.* 17: 520–527.

D'Souza-Schorey, C. and Chavrier, P. (2006) ARF proteins: roles in membrane traffic and beyond. *Nat. Rev. Mol. Cell Biol.* 7: 347–358.

Feraru, E., Feraru, M.I., Asaoka, R., Paciorek, T., De Rycke, R., Tanaka, H. et al. (2012) BEX5/RabA1b regulates trans-Golgi network-to-plasma membrane protein trafficking in Arabidopsis. *Plant Cell* 24: 3074–3086.

Furutani, M., Vernoux, T., Traas, J., Kato, T., Tasaka, M. and Aida, M. (2004) PIN-FORMED1 and PINOID regulate boundary formation and cotyledon development in Arabidopsis embryogenesis. *Development* 131: 5021–5030.

Gälweiler, L., Guan, C., Müller, A., Wisman, E., Mendgen, K., Yephremov, A. et al. (1998) Regulation of polar auxin transport by AtPIN1 in *Arabidopsis* vacular tissue. *Science* 282: 2226–2230.

Geldner, N., Anders, N., Wolters, H., Keicher, J., Kornberger, W., Muller, P. et al. (2003) The Arabidopsis GNOM ARF-GEF mediates endosomal recycling, auxin transport, and auxin-dependent plant growth. *Cell* 112: 219–230.

Geldner, N., Friml, J., Stierhof, Y., Jürgens, G. and Palme, K. (2001) Auxin transport inhibitors block PIN1 cycling and vesicle trafficking. *Nature* 413: 425–428.

Hardtke, C. and Berleth, T. (1998) The Arabidopsis gene MONOPTEROS encodes a transcription factor mediating embryo axis formation and vascular development. *EMBO J.* 17: 1405–1411.

Jones, S., Newman, C., Liu, F. and Segev, N. (2000) The TRAPP complex is a nucleotide exchanger for Ypt1 and Ypt31/32. *Mol. Biol. Cell* 11: 4403–4411.

Kitakura, S., Vanneste, S., Robert, S., Lofke, C., Teichmann, T., Tanaka, H. et al. (2011) Clathrin mediates endocytosis and polar distribution of PIN auxin transporters in Arabidopsis. *Plant Cell* 23: 1920–1931.

Kleine-Vehn, J., Huang, F., Naramoto, S., Zhang, J., Michniewicz, M., Offringa, R. et al. (2009) PIN auxin efflux carrier polarity is regulated by PINOID kinase-mediated recruitment into GNOM-independent trafficking in Arabidopsis. *Plant Cell* 21: 3839–3849.

Kleine-Vehn, J., Wabnik, K., Martiniere, A., Langowski, L., Willig, K., Naramoto, S. et al. (2011) Recycling, clustering, and endocytosis jointly maintain PIN auxin carrier polarity at the plasma membrane. *Mol. Syst. Biol.* 7: 540.

Koizumi, K., Naramoto, S., Sawa, S., Yahara, N., Ueda, T., Nakano, A. et al. (2005) VAN3 ARF-GAP-mediated vesicle transport is involved in leaf vascular network formation. *Development* 132: 1699–1711.

Koizumi, K., Sugiyama, M. and Fukuda, H. (2000) A series of novel mutants of Arabidopsis thaliana that are defective in the formation of continuous vascular network: calling the auxin signal flow canalization hypothesis into question. *Development* 127: 3197–3204.

Kubo, M., Udagawa, M., Nishikubo, N., Horiguchi, G., Yamaguchi, M., Ito, J. et al. (2005) Transcription switches for protoxylem and metaxylem vessel formation. *Genes Dev.* 19: 1855–1860.

Mattsson, J., Sung, Z. and Berleth, T. (1999) Responses of plant vascular systems to auxin transport inhibition. *Development* 126: 2979–2991.

Morozova, N., Liang, Y., Tokarev, A., Chen, S., Cox, R., Andrejic, J. et al. (2006) TRAPPII subunits are required for the specificity switch of a Ypt-Rab GEF. *Nat. Cell Biol.* 8: 1263–1269.

Naramoto, S., Kleine-Vehn, J., Robert, S., Fujimoto, M., Dainobu, T., Paciorek, T. et al. (2010) ADP-ribosylation factor machinery mediates endocytosis in plant cells. *Proc. Natl. Acad Sci. USA* 107: 21890–21895.

Naramoto, S., Sawa, S., Koizumi, K., Uemura, T., Ueda, T., Friml, J. et al. (2009) Phosphoinositide-dependent regulation of VAN3 ARF-GAP localization and activity essential for vascular tissue continuity in plants. *Development* 136: 1529–1538.

Nelson, T. and Dengler, N. (1997) Leaf vascular pattern formation. *Plant Cell* 9: 1121–1135.

Paciorek, T., Sauer, M., Balla, J., Wiśniewska, J. and Friml, J. (2006) Immunocytochemical technique for protein localization in sections of plant tissues. *Nat. Protoc.* 1: 104–107.

Petrášek, J., Mravec, J., Bouchard, R., Blakeslee, J., Abas, M., Seifertová, D. et al. (2006) PIN proteins perform a rate-limiting function in cellular auxin efflux. *Science* 312: 914–918.

Qi, X. and Zheng, H. (2011) Arabidopsis TRAPPII is functionally linked to Rab-A, but not Rab-D in polar protein trafficking in trans-Golgi network. *Plant Signal. Behav.* 6: 1679–1683.

Qi, X.Y., Kaneda, M., Chen, J., Geitmann, A. and Zheng, H.Q. (2011) A specific role for Arabidopsis TRAPPII in post-Golgi trafficking that is crucial for cytokinesis and cell polarity. *Plant J.* 68: 234–248.

Robert, S., Kleine-Vehn, J., Barbez, E., Sauer, M., Paciorek, T., Baster, P. et al. (2010) ABP1 mediates auxin inhibition of clathrin-dependent endocytosis in Arabidopsis. *Cell* 143: 111–121.

Sacher, M., Kim, Y., Lavie, A., Oh, B. and Segev, N. (2008) The TRAPP complex: insights into its architecture and function. *Traffic* 9: 2032–2042.

Sachs, T. (1981) The control of the patterned differentiation of vascular tissues. *Adv. Bot. Res.* 9: 151–262.

Sachs, T. (1989) The development of vascular networks during leaf development. *Curr. Top. Plant Biochem. Physiol.* 8: 168–183.

Sachs, T. (1991) Cell polarity and tissue patterning in plants. *Development* 113: 83–93.

Sachs, T. (2000) Integrating cellular and organismic aspects of vascular differentiation. *Plant Cell Physiol.* 41: 649–656.

Scarpella, E., Marcos, D., Friml, J. and Berleth, T. (2006) Control of leaf vascular patterning by polar auxin transport. *Genes Dev.* 20: 1015–1027.

Shevell, D., Kunkel, T. and Chua, N. (2000) Cell wall alterations in the arabidopsis emb30 mutant. *Plant Cell* 12: 2047–2060.

Sieburth, L.E. (1999) Auxin is required for leaf vein pattern in Arabidopsis. *Plant Physiol.* 121: 1179–1190.

Sieburth, L., Muday, G., King, E., Benton, G., Kim, S., Metcalf, K. et al. (2006) SCARFACE encodes an ARF-GAP that is required for normal auxin efflux and vein patterning in Arabidopsis. *Plant Cell* 18: 1396–1411.

Tanaka, H., Kitakura, S., De Rycke, R., De Groodt, R. and Friml, J. (2009) Fluorescence imaging-based screen identifies ARF GEF component of early endosomal trafficking. *Curr. Biol.* 19: 391–397.

Tian, G.W., Mohanty, A., Chary, S.N., Li, S., Paap, B., Drakaki, G. et al. (2004) High-throughput fluorescent tagging of full-length Arabidopsis gene products in planta. *Plant Physiol.* 135: 25–38.

Ueda, T., Yamaguchi, M., Uchimiya, H. and Nakano, A. (2001) Ara6, a plant-unique novel type Rab GTPase, functions in the endocytic pathway of Arabidopsis thaliana. *EMBO J.* 20: 4730–4741.

Wee, E., Sherrier, D., Prime, T. and Dupree, P. (1998) Targeting of active sialyltransferase to the plant Golgi apparatus. *Plant Cell* 10: 1759–1768.

Wiśniewska, J., Xu, J., Seifertová, D., Brewer, P., Růžička, K., Blilou, I. et al. (2006) Polar PIN localization directs auxin flow in plants. *Science* 312: 883.

Yamasaki, A., Menon, S., Yu, S., Barrowman, J., Meerloo, T., Oorschot, V. et al. (2009) mTrs130 is a component of a mammalian TRAPPII complex, a Rab1 GEF that binds to COPI-coated vesicles. *Mol. Biol. Cell* 20: 4205–4215.

Zerial, M. and McBride, H. (2001) Rab proteins as membrane organizers. *Nat. Rev. Mol. Cell Biol.* 2: 107–117.